# Delineation of Structural Domains in Eukaryotic 5S rRNA with a Rhodium Probe†

Christine S. Chow,‡ Kevin M. Hartmann,§ Stephen L. Rawlings,§ Paul W. Huber,§ and Jacqueline K. Barton*,‡

*Division of Chemistry and Chemical Engineering, California Institute of Technology, Pasadena, California 91125, and Department of Chemistry and Biochemistry, University of Notre Dame, Notre Dame, Indiana 46556*

*Received November 6, 1991; Revised Manuscript Received January 14, 1992*

ABSTRACT: The three-dimensional folding of *Xenopus* oocyte 5S rRNA has been examined using the coordination complex $Rh(phen)_2phi^{3+}$ (phen = phenanthroline; phi = phenanthrenequinone diimine) as a structural probe. $Rh(phen)_2phi^{3+}$ binds neither double-helical RNA nor unstructured single-stranded regions of RNA. Instead, the complex targets through photoactivated cleavage sites of tertiary interaction which are open in the major groove and accessible to stacking. The sites targeted by the rhodium complex have been mapped on the wild-type *Xenopus* oocyte RNA, on a truncated RNA representing the arm of the molecule comprised of helix IV–loop E–helix V, and on several single-nucleotide mutants of the 5S rRNA. On the wild-type 5S rRNA, strong cleavage is found at residues U73, A74, A101, and U102 in the E loop and U80 and G81 in helix IV; additional sites are evident at A22 and A56 in the B loop, C29 and A32 in helix III, and C34, C39, A42, and C44 in the C loop. Given the similarity observed in cleavage between the full 5S RNA and the truncated fragment as well as the absence of any long-range effects on cleavage in mutant RNAs, the results do not support models which involve long-range tertiary interactions. Cleavage results with $Rh(phen)_2phi^{3+}$ do, however, indicate that the apposition of several noncanonical bases as well as stem–loop junctions may result in intimately stacked structures with opened major grooves. In particular, on the basis of cleavage results on mutant RNAs, both loops C and E represent structures where the strands constituting each loop are not independent of one another but are intrinsically structured. Stem–loop junctions, helix bulges containing more than one unmatched nucleotide, and a U-U mismatch also appear to provide open major grooves for targeting by $Rh(phen)_2phi^{3+}$. These distinctive structures may also be utilized for specific recognition by proteins, such as the transcription factor TFIIIA, that bind to 5S rRNA.

Ribosomal 5S RNA is an essential component of the ribosome, yet, despite extensive study, the individual function and the higher order structure of this small RNA (120 nucleotides) is still not known with precision. On the basis of comparative sequence analysis, Fox and Woese (1975) first suggested a minimal secondary structure for prokaryotic 5S rRNA containing four helices, two internal loops, and two external loops. The same strategy was used later to arrive at a similar model for eukaryotic 5S rRNA but with the addition of a fifth helix and an added internal loop (Luehrsen & Fox, 1981). Chemical and enzymatic assays of polymer structure as well as several spectroscopic studies are all consistent with this basic model for the secondary structure of prokaryotic and eukaryotic 5S rRNAs (Andersen et al., 1984; Christiansen et al., 1987; Romaniuk et al., 1988). Certain regions of the RNA molecule have nonetheless remained refractory to analysis, and the overall three-dimensional structure of the molecule remains ill-defined.

The three-dimensional folding of the structurally well-characterized yeast $tRNA^{Phe}$ (Kim et al., 1974; Quigley & Rich, 1976) is found to depend upon a complex network of hydrogen bonds and base stacking interactions that vary substantially from a Watson–Crick hydrogen-bonded double helix. We will consider here for clarity all such interactions as tertiary. What tertiary interactions are present and define the folding of 5S rRNA? Secondary structure maps for *Xenopus* oocyte 5S rRNA suggest that the RNA should contain bulged and unusual mismatched residues in helices II, III, and V. Several tentative models for 5S rRNA tertiary structure have described a folded structure containing long-range interactions between loop C and either the internal loop E or external loop D (Böhm et al., 1981; Hancock & Wagner, 1982; Pieler & Erdmann, 1982; Nazar, 1991) or pseudoknot structures (Göringer & Wagner, 1986). There is also evidence that suggests that 5S rRNAs are flexible and can undergo conformational switches which may have functional importance (Kao & Crothers, 1980; Kime & Moore, 1982). This flexibility may account for some of the discrepancies between the various models for tertiary folding proposed. Westhof et al. (1989) have developed a model for higher order structure that can accommodate both eubacterial (spinach chloroplast) and eukaryotic (*Xenopus*) 5S rRNA. This structure does not possess any long-range tertiary interactions between the loops, but it involves instead short-range interactions within the internal loop regions. In this model, the 5S rRNA adopts a distorted Y-shape structure with three independent domains which contain several noncanonical base pairs (A-A, U-U, and A-G) within the internal loop regions and bulged nucleotides within the helical regions. Growing evidence indicates the importance of RNA structural variations, such as loop structures and bulged nucleotides, as key elements in the recognition of RNA by proteins (Peattie et al., 1981; Christiansen et al., 1985; Mougel et al., 1987; Rould et al., 1989; Calnan et al., 1991; Ruff et al., 1991; Weeks & Crothers, 1991).

Photoactivation of the transition metal complex bis(phenanthroline)(phenanthrenequinone diimine)rhodium(III) [$Rh(phen)_2(phi)^{3+}$] promotes strand cleavage at accessible sites

† We are grateful for the financial support of the NIH (GM33309 to J.K.B.; GM38200 to P.W.H.). In addition, C.S.C. thanks the Parsons Foundation for their fellowship support.

* To whom correspondence should be addressed.

‡ California Institute of Technology.

§ University of Notre Dame.

0006-2960/92/0431-3534$03.00/0 

in the major groove of DNA and RNA. The rhodium complex, which binds to double-helical DNA by intercalation in the major groove (Pyle et al., 1989, 1990)

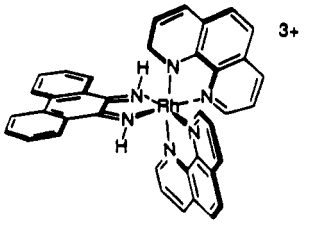

yields no cleavage in the double-helical regions of tRNA or in unstructured single-stranded regions (Chow & Barton, 1990; Chow et al., 1992). Instead, $Rh(phen)_2(phi)^{3+}$ appears to target preferentially regions of tertiary structure in tRNAs which are structured so that the major grooves are open and accessible to stacking by the complex. Thus, this complex has proven to be a valuable probe for higher order structure in RNA. $Rh(phen)_2(phi)^{3+}$ is used here to examine the three-dimensional structure of *Xenopus* oocyte 5S rRNA. Rhodium cleavage has been mapped on several single-nucleotide mutants of 5S rRNA and on truncated RNA representing the arm of the molecule comprised of helix IV–loop E–helix V. The results do not support models which involve long-range tertiary interactions. However, cleavage by $Rh(phen)_2phi^{3+}$ at specific sites indicates that the apposition of several noncanonical bases found in 5S rRNA as well as stem–loop junctions may result in intimately stacked structures with opened major grooves. These distinctive structures with accessible bases may be utilized for specific recognition by proteins, such as the transcription factor TFIIIA, that bind to this RNA.

## Materials and Methods

*In Vitro Synthesis of 5S rRNAs.* The recombinant plasmid pT75S contains a T7 RNA polymerase promoter immediately upstream of a *Xenopus* oocyte 5S rRNA gene inserted into the vector pUC119 (Rawlings & Huber, 1992). The procedures for oligonucleotide-directed mutagenesis and in vitro synthesis of the 5S rRNAs by runoff transcription have been described (Rawlings & Huber, 1992).

*Synthesis and Purification of a Truncated Fragment of Xenopus Oocyte 5S rRNA (3′Δ12–5′Δ64).* The oligoribonucleotide (45-mer) based on domain 3 of the *Xenopus* oocyte 5S rRNA (3′Δ12–5′Δ64) was synthesized using T7 RNA polymerase and synthetic DNA templates following the procedure of Milligan et al. (1987). DNA templates were synthesized on a Pharmacia Gene Assembler using the phosphoramidite method. The DNA templates were purified by the Nensorb preparative purification method (Johnson et al., 1990) followed by polyacrylamide gel electrophoresis (8 M denaturing). The purified DNA was stored in 10 mM Tris-HCl, pH 7.0, at −20 °C. The DNA templates were freshly annealed by heating the two strands together to 100 °C for 10 min and slow cooling over a 6-h period to +4 °C. The following DNA templates were used:

```
5'- TAATA CGACT CACTA TAG -3'

3'- ATTAT GCTGA GTGAT ATCCG GACCA ATCAT GGACC
    TACCC TCTGG CGGAC CCTTA TGGTC CA -5'
```

The transcript reaction mixture contained 40 mM Tris-HCl (pH 8.1 at 37 °C), 2 mM spermidine, 5 mM dithiothreitol, 50 μg/mL bovine serum albumin, 0.01% (v/v) Triton X-100, 1 mM NTPs, 6 mM $MgCl_2$, 200 nmol of DNA template, and 30 units/μL T7 RNA polymerase and was incubated for 2 h at 37 °C. Following the transcription reaction, the synthesized RNA 45-mer was purified by the Nensorb purification method (Johnson et al., 1986) and stored in 10 mM Tris-HCl, pH 7.5.

*Preparation of Labeled Wild-Type and Mutant 5S rRNAs.* The RNAs were labeled either at the 3′-end with cytidine 3′,5′-[5′-$^{32}$P]bisphosphate using T4 RNA ligase (England & Uhlenbeck, 1978) or at the 5′-end with [γ-$^{32}$P]ATP using T4 polynucleotide kinase (Silberklang et al., 1977). The radioactive RNAs were gel purified on 15% denaturing polyacrylamide gels, located by autoradiography, excised, and eluted from the gel slices in 45 mM Tris, 45 mM boric acid, 1.25 mM EDTA, pH 8.0. The eluted RNAs were precipitated twice with ethanol and stored in 10 mM Tris-HCl, pH 7.5.

*Cleavage of 5S rRNAs by $Rh(phen)_2phi^{3+}$.* $Rh(phen)_2phi^{3+}$ stock solutions were freshly prepared. All end-labeled rRNAs were renatured by heating to 65 °C for 10 min in 10 mM Tris-HCl, 10 mM $MgCl_2$, 300 μM KCl, pH 7.5, and slow cooling to room temperature prior to use. A typical 20-μL reaction mixture contained 50 mM sodium cacodylate, pH 7.0, labeled 5S rRNA, and 10 μM $Rh(phen)_2phi^{3+}$. The final concentration of nucleotides was adjusted to 100 μM by the addition of carrier tRNA. Irradiation for 10 min at 365 nm at ambient temperature using a 1000-W Hg/Xe lamp and monochromator yielded site-specific cleavage of the 5S rRNA samples only in the presence of the rhodium complex. The reaction mixtures were precipitated with ethanol and washed several times with 70% ethanol to remove traces of salt before analysis on sequencing gels.

*Sequencing Gels.* The rhodium cleavage products were analyzed on 15% polyacrylamide gels containing 8 M urea. The full-length 5S rRNAs and cleavage products were identified by coelectrophoresing the appropriate chemical sequencing reactions (Peattie, 1979) and viewed by autoradiography. Reactions with dimethyl sulfate followed by $NaBH_4$ treatment, diethyl pyrocarbonate, and hydrazine yield specific cleavages at G, A, and U residues, respectively, with 5′- and 3′-phosphate termini. Fragments produced by $Rh(phen)_2phi^{3+}$ cleavage also possess 5′- and 3′-phosphate termini and may therefore be compared directly with the chemical sequencing lanes.

## Results

*Cleavage of Xenopus Oocyte Wild-Type 5S rRNA by $Rh(phen)_2phi^{3+}$.* The sites of $Rh(phen)_2phi^{3+}$ induced strand scission of wild-type 5S rRNA from *Xenopus* oocytes were determined using 5′- and 3′-end-labeled RNAs. As can be seen in Figure 1A, few and specific sites of cleavage by the rhodium complex are evident on the 3′-end-labeled 5S rRNA. Strong cleavage occurs at residues U73, A74, A101, and U102 in the E loop and U80 and G81 in helix IV; weak cleavage occurs at A100 in loop E and A103 in helix V. In polyacrylamide gels which are further resolved, additional sites are evident at A22 and A56 in the B loop, C29 and A32 in helix III, and C34, C39, A42, and C44 in the C loop. Identical sites of cleavage are observed in experiments conducted with 5′-end-labeled 5S rRNA. In addition, identical sites of cleavage are observed whether the samples are renatured with low (300 μM) or high (300 mM) KCl concentrations. Figure 2 displays sites of rhodium cleavage on the map of the secondary structure of the *Xenopus* oocyte 5S rRNA.

With the exception of C39, the rhodium cleavage sites occur exclusively at stem–loop junctions, mismatched base pairs, or bulged residues. These results are consistent with cleavage results found earlier on $tRNA^{Phe}$, in which the rhodium complex does not cleave in double-helical regions or in unstructured single-stranded regions of the RNA (Chow & Barton, 1990). Instead, cleavage on $tRNA^{Phe}$ and $tRNA^{Asp}$ is limited to sites

Table I: Cleavage of 5S rRNA Mutants by $Rh(phen)_2phi^{3+}$

| mutant | diminished sites[a] | enhanced sites[a] | no change[a] |
|---|---|---|---|
| U43A-C44G | A32, C34, C39, G44 | | B loop, E loop, helix IV |
| A42C | C34, C39, C42, C44 | A32, C36 | B loop, E loop, helix IV |
| A100C | | A101, U102, A103, U73, A74 | B loop, C loop, helix IV |
| A101U | | U101, U102, A103, U73, A74 | B loop, C loop, helix IV |
| A74C | A101, U102, A103 | U73, C74 | B loop, C loop, helix IV |
| A74G | A101, U102, A103 | U73, G74 | B loop, C loop, helix IV |
| ΔA83 | | | B loop, C loop, E loop, helix IV |
| U96A | U80, G81 | | B loop, C loop, E loop |
| U96G-ΔA83 | U80, G81 | | B loop, C loop, E loop |
| U96A-ΔA83 | U80, G81 | | B loop, C loop, E loop |
| G81C-C95G | | U80, C81 | B loop, C loop, E loop |
| Δ1–64, Δ110–121 | | | E loop, helix IV |

[a] Cleavage relative to wild-type 5S RNA from *Xenopus* oocytes.

involved in tertiary interactions such as triple-base interactions, stem–loop junctions, or structured loop regions (Chow et al., 1992). The rhodium cleavage results on 5S rRNA support the minimal secondary structure model proposed by Luehrsen and Fox (1981) since no cleavage by $Rh(phen)_2phi^{3+}$ is apparent in the proposed double-stranded regions. In addition, since the rhodium complex does not promote strand scission at purely single-stranded regions, the cleavage data suggest that the loop regions of the 5S rRNA must be structured, involving either non-Watson–Crick base pairing within the loops or long-range tertiary interactions between the loop regions. Cleavage at the U-U mismatch and at the site adjacent to an AA bulge are also suggestive of structures which are different from canonical A-form RNA double helices.

*Cleavage of a Truncated Fragment of Xenopus Oocyte 5S rRNA (3′Δ12–5′Δ64) by $Rh(phen)_2phi^{3+}$.* Because several models for the tertiary structure of 5S rRNA include long-range contacts between the two "arms" of the molecule, it became necessary to establish whether such contacts might account for the cleavage pattern obtained with $Rh(phen)_2phi^{3+}$. A smaller fragment of the 5S rRNA, constituting a single "arm", was therefore synthesized (Figure 2, insert), and cleavage by the rhodium complex was examined and compared to that on the full 5S rRNA. If $Rh(phen)_2phi^{3+}$ is recognizing long-range tertiary interactions between the loop regions, as in tRNA (Chow et al., 1992), then deletion of the B and C loops should lead to an altered cleavage by the rhodium complex. Conversely, if the E loop has some intrinsic structure which is independent of the rest of the molecule, then the cleavage specificity of the rhodium complex should remain the same.

The truncated RNA fragment corresponding to residues G65 to U109 of the full-length 5S rRNA was synthesized by in vitro transcription by T7 RNA polymerase from a synthetic DNA template. As shown in Figure 1B, the cleavage pattern for the truncated 5S rRNA is nearly identical to that obtained for wild-type 5S rRNA. Strong cleavage by $Rh(phen)_2phi^{3+}$ on the 3′Δ12–5′Δ64 mutant is observed at U80, A100, and U102 with minor cleavage at U73, A74, A101, and A103. Changes in rhodium cleavage at G81, A100, and A101 are evident. Nonetheless, it is clear from these results that, despite subtle differences, the same regions on the truncated fragment as on the full 5S rRNA are recognized. The 5S rRNA fragment therefore likely adopts the same conformation as the corresponding region in the full-length 5S rRNA. These results are therefore consistent with a structure for helix IV and loop E which is independent of the rest of the 5S rRNA molecule.

*Cleavage of 5S rRNA Mutants by $Rh(phen)_2phi^{3+}$.* The preceding results indicate the absence of long-range tertiary interactions in the molecule and suggest instead that cleavage by $Rh(phen)_2phi^{3+}$ arises from the recognition of tertiary structures generated more locally by flanking and opposing bases. To confirm the absence of long-range tertiary interactions in the 5S RNA and to probe further the sites recognized by the metal complex, several substitutions at positions in helix IV and loops C and E were made and their effects on cleavage by $Rh(phen)_2phi^{3+}$ were determined. A series of 5S rRNA mutants were prepared by in vitro transcription with T7 RNA polymerase. The cleavage data given in Figure 3, obtained on 3′-end-labeled 5S rRNA, show the effects of mutations on cleavage in loops C and E as well as helix IV. Cleavage data for loops B and C were obtained on 5′-end-labeled RNA (data not shown). The results for all mutations

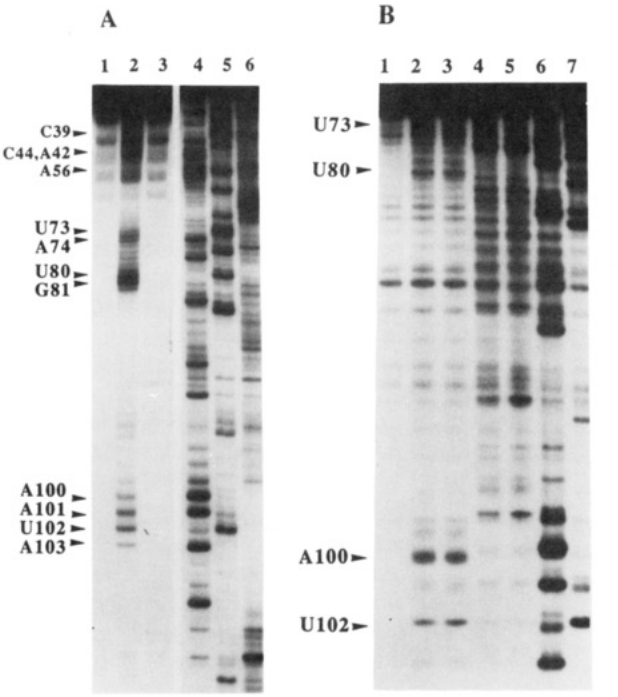


FIGURE 1: Cleavage of *Xenopus* oocyte 5S rRNA and a truncated version by $Rh(phen)_2phi^{3+}$. (A) Autoradiogram showing cleavage of the full 5S rRNA in 50 mM sodium cacodylate, pH 7.0. Lane 1: labeled RNA without metal or irradiation. Lane 2: cleaved RNA after incubation with $Rh(phen)_2phi^{3+}$ and irradiation. Lane 3: labeled RNA irradiated in the absence of metal complex. Lanes 4–6: A-, U-, and G-specific reactions, respectively. (B) Autoradiogram showing cleavage of the truncated 5S rRNA (3′Δ12–5′Δ64) by $Rh(phen)_2phi^{3+}$ in 50 mM sodium cacodylate, pH 7.0. Lane 1: labeled RNA without metal or irradiation. Lanes 2 and 3: cleaved RNA after incubation with $Rh(phen)_2phi^{3+}$ and irradiation. Lanes 4 and 5: G-specific reaction. Lanes 6 and 7: A- and U-specific reactions, respectively. Major sites of cleavage are marked.

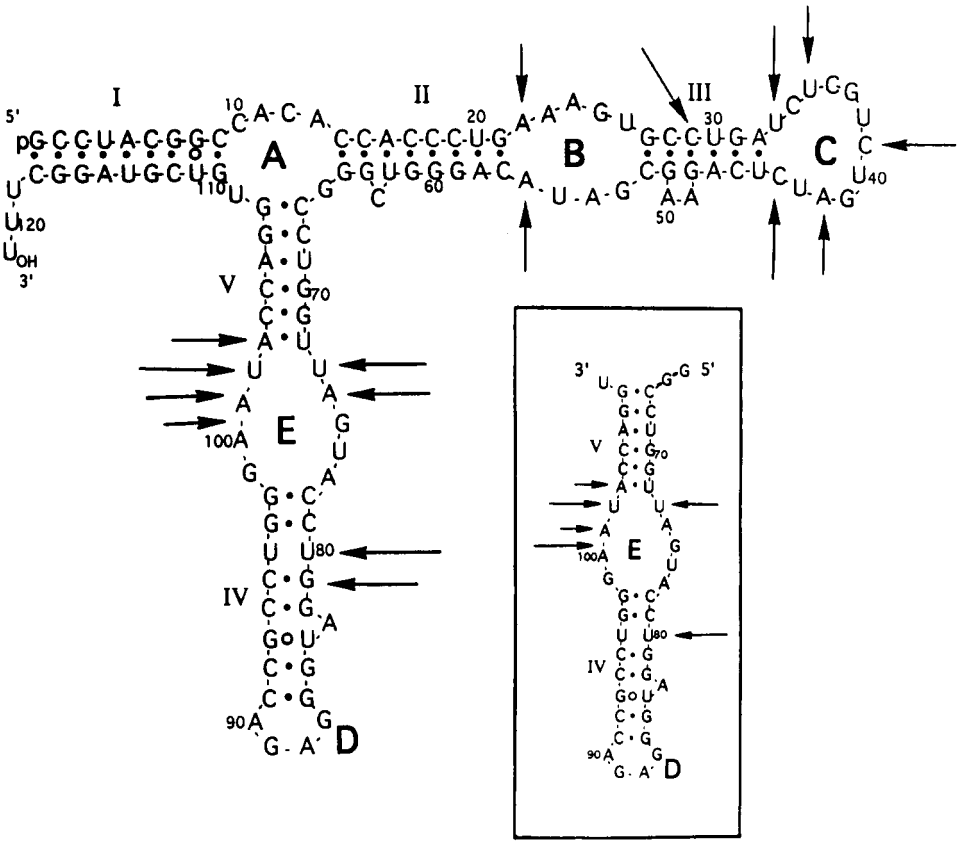


FIGURE 2: Schematic illustration of the secondary structure of *Xenopus* 5S rRNA with designations of the sites of cleavage by $Rh(phen)_2phi^{3+}$. The arrows indicate the positions of $Rh(phen)_2phi^{3+}$ promoted strand scission with length corresponding to relative cleavage intensity. The boxed insert illustrates cleavage on the truncated *Xenopus* oocyte 5S rRNA (3′Δ12–5′Δ64) by $Rh(phen)_2phi^{3+}$.

are shown schematically in Figure 4 and summarized in Table I.

The substitutions in loop C produce no changes in cleavage by the rhodium complex in loops B and E or in helices III and IV relative to the cleavage observed on wild-type 5S rRNA. However, there are variations in cleavage by $Rh(phen)_2phi^{3+}$ observed within the C loop. The mutation U43A-C44G leads to diminished cleavage in the C loop at sites A32 and G44 and complete loss at C34 and C39. Similarly, the mutant A42C exhibits diminished cleavage at C42 with complete loss at C34, C39, and C44, but enhanced cleavage at A32 and an additional cleavage site at C36. The E loop mutants yield no long-range changes in cleavage in the B or C loops or in helices III and IV. For the mutation A100C, enhanced cleavage is observed at U73, A74, A101, U102, and A103, however. Similarly, the mutation A101U leads to enhanced cleavage by the rhodium complex at U73, A74, U101, U102, and A103. Mutations made on the 5′-side of the E loop (A74C and A74G) lead to a diminished cleavage on the opposite side of the loop at A101, U102, and A103 but exhibit a concomitant increase in cleavage at U73, adjacent to the site of mutation, as well as at residue 74. The changes observed in cleavage by the rhodium complex with mutations in loops E and C of the 5S rRNA establish that the loop regions of the molecule contain intrinsic structures which are recognized by $Rh(phen)_2phi^{3+}$. One may furthermore conclude, on the basis of these data, that no long-range interactions exist among loops C and E and helix IV.

Lastly, the introduction of mutations in helix IV leads to alterations in cleavage by $Rh(phen)_2phi^{3+}$ which are restricted to helix IV. No changes in rhodium cleavage are observed in the loop regions or in helix III for these mutants. Inspection of the secondary structure map for the wild-type 5S rRNA would suggest that cleavage by the rhodium complex at U80 and G81 of helix IV might arise owing to a structural deformation in the helix caused by the bulged nucleotide at position 83 and/or the U-U mismatch. A deletion of the bulged A83 results in a cleavage pattern for the rhodium complex which is identical at all sites to that found on the wild-type 5S rRNA. However, if the U-U mismatch is changed to an A-U Watson–Crick base pair, cleavage is no longer observed at either U80 or G81. If the U-U mismatch is changed to either a G-U mismatch or an A-U base pair with the deletion of A83, no cleavage is evident at U80 or G81. Interestingly, if the neighboring C95-G81 base pair is switched to a G95-C81 base pair, cleavage at U80 and C81 is enhanced compared to the wild-type 5S rRNA cleavage. These results indicate that the U-U mismatch rather than the bulged A residue leads to the structural distortion recognized by the rhodium complex. In addition, the flanking C-G base pair has an effect on the specific structure which is recognized; the change in cleavage intensity at the U-U mismatch seen by inverting the flanking base pair likely reflects subtle modifications in the nucleotide stacking interactions.

## Discussion

*Recognition Characteristics of $Rh(phen)_2phi^{3+}$.* The reaction of $Rh(phen)_2phi^{3+}$ with *Xenopus* oocyte 5S rRNA does not occur at double-helical regions of the molecule or within purely single-stranded regions or canonical stem structures. Instead, cleavage by the rhodium complex on 5S rRNA is apparent in loop regions, stem–loop junctions, base pair mismatches, and bulged residues. These results may be understood on the basis of the DNA recognition characteristics of $Rh(phen)_2phi^{3+}$. Since the rhodium complex interacts in the major groove of DNA by intercalation, stacking by the

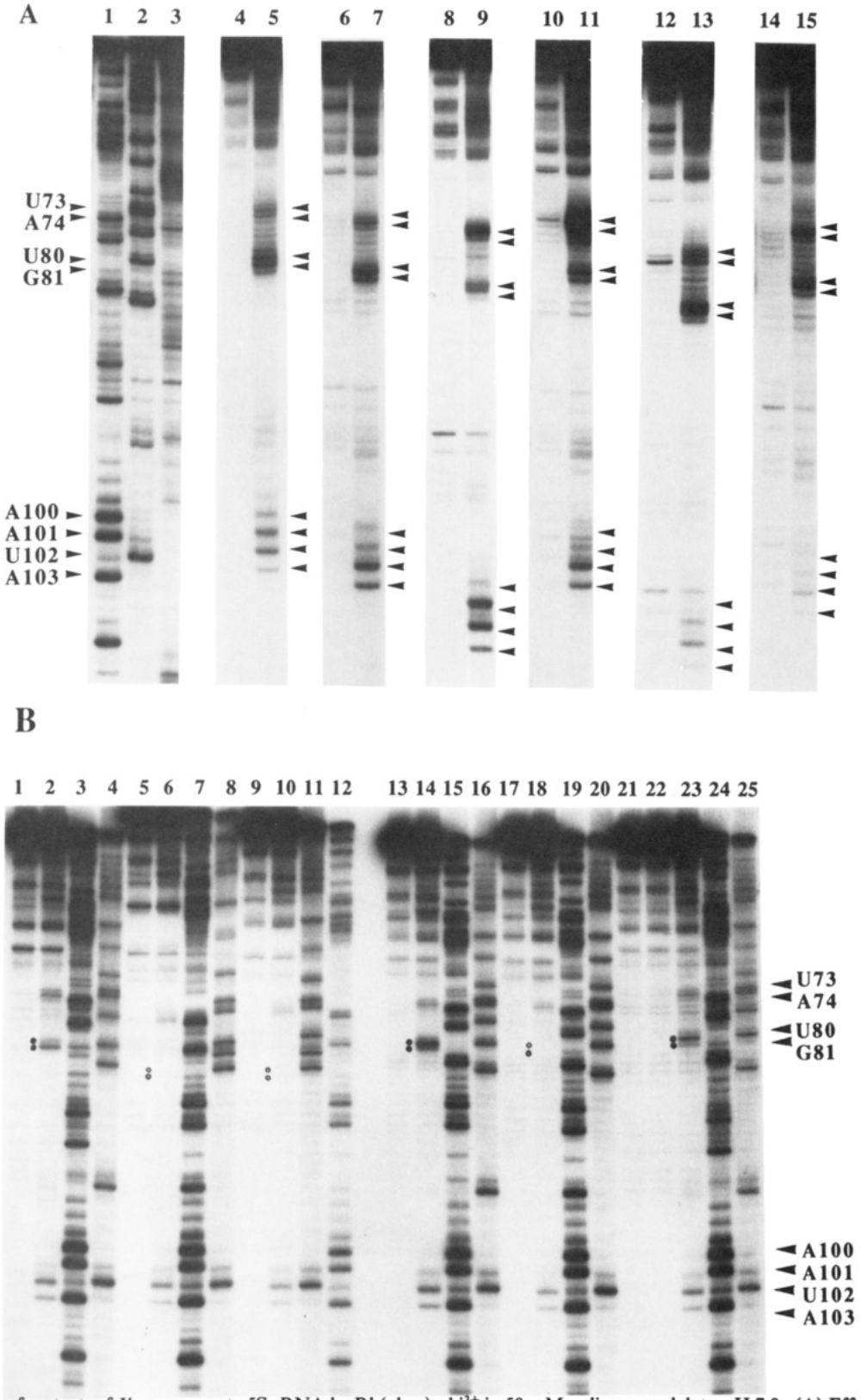


FIGURE 3: Cleavage of mutants of *Xenopus* oocyte 5S rRNA by $Rh(phen)_2phi^{3+}$ in 50 mM sodium cacodylate, pH 7.0. (A) Effects of mutations on cleavage in the E and C loops. Lanes 1–3: A-, U-, and G-specific reactions on wild-type (WT) 5S rRNA. Lanes 4, 6, 8, 10, 12, and 14: control end-labeled RNAs in the absence of metal and light; WT, U43A-C44G, A100C, A101U, A74C, and A74G, respectively. Lanes 5, 7, 9, 11, 13, and 15: cleavage by $Rh(phen)_2phi^{3+}$ of WT, U43A-C44G, A100C, A101U, A74C, and A74G, respectively. Major sites of cleavage are marked. The mutant RNAs were electrophoresed on separate gels next to sequencing lanes, which explains the different mobilities, but are shown here together for comparison. For ease of comparison, only the cleavage lanes and control lanes are shown. (B) Effects of mutations on cleavage in helix IV. Lanes 1, 5, 9, 13, 17, and 21: control end-labeled RNAs without metal or irradiation; ΔA83, U96A-ΔA83, U96G-ΔA83, G81C-C95G, U96A, and WT, respectively. Lanes 2, 6, 10, 14, 18, and 23: specific cleavage by $Rh(phen)_2phi^{3+}$ on ΔA83, U96A-ΔA83, U96G-ΔA83, G81C-C95G, U96A, and WT, respectively. Lanes 3, 7, 12, 15, 19, and 24: A-specific reactions on ΔA83, U96A-ΔA83, U96G-ΔA83, G81C-C95G, U96A, and WT, respectively. Lanes 4, 8, 11, 16, 20, and 25: U-specific reactions on ΔA83, U96A-ΔA83, U96G-ΔA83, G81C-C95G, U96A, and WT, respectively. Lane 22: end-labeled WT irradiated in the absence of metal. Major sites of cleavage are marked. Filled circles indicate cleavage in helix IV (U80, G81). These sites have different mobilities for each mutant due to the difference of one nucleotide for the deletion mutants. The open circles indicate the lack of cleavage at the same sites (U80, G81) in helix IV.

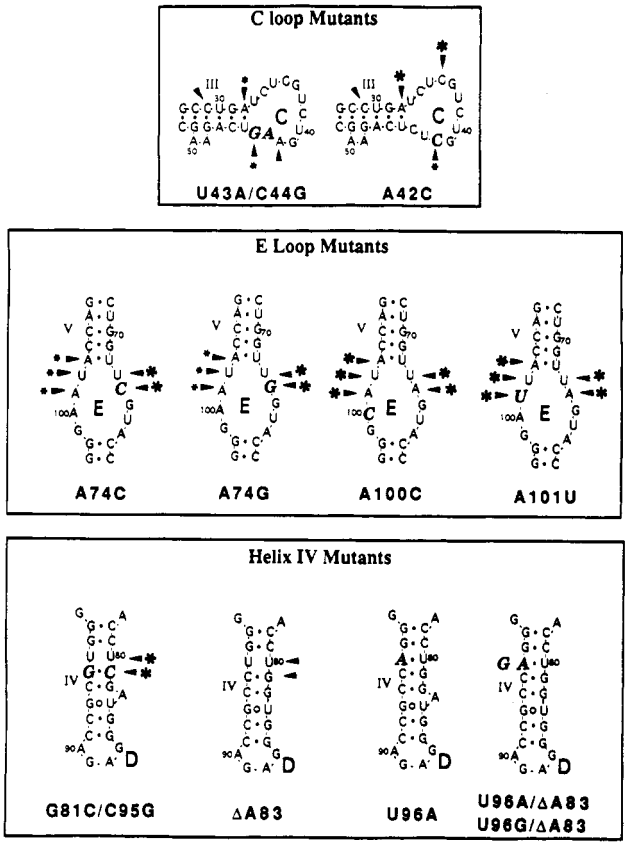


FIGURE 4: Schematic illustrations of Rh(phen)$_2$phi$^{3+}$ cleavage on *Xenopus* 5S rRNA mutants. The arrowheads indicate the positions of strand scission promoted by Rh(phen)$_2$phi$^{3+}$. The cleavage intensity at the marked site is the same as with wild type unless noted by an asterisk. A large asterisk indicates that cleavage is enhanced relative to that of wild type, while a small asterisk indicates that cleavage is diminished relative to that of wild type.

complex in the deep and narrow major groove of double-helical RNA is not expected on the basis of steric considerations. The complex could stack easily, however, at sites which are more opened in the major groove. In crystallographically characterized tRNAs, it has been found that Rh(phen)$_2$phi$^{3+}$ cleaves preferentially at regions of tertiary interactions; these regions are structured so as to provide a major groove which is open and accessible to stacking by the metal complex (Chow et al., 1992).

Cleavage by Rh(phen)$_2$phi$^{3+}$ on 5S rRNA appears to be consistent with the sites of cleavage found earlier on tRNA. The sites which are recognized do not appear to be involved in long-range tertiary folding, however. Instead the sites recognized on *Xenopus* oocyte 5S rRNA represent several families of localized tertiary interactions, including stem–loops, structured loops, and sites with mismatched bases.

*The Y-Shape Structure.* We have examined cleavage on a series of 5S rRNA mutants and a truncated 5S rRNA in order to test the involvement of the cleaved regions in long-range tertiary interactions; such recognition by the rhodium complex was found to be important on tRNA. These data, summarized in Figures 2 and 4 as well as Table I, indicate that the domains of the *Xenopus* oocyte 5S rRNA are independently organized. Mutations in either the loop regions or helical region affect the structure near the site of substitution, but there are no long-range effects found at distant positions. In addition, the cleavage pattern on the truncated 5S rRNA (3′Δ12–5′Δ64) is nearly identical to that of the native molecule in loop E and helix IV. Therefore, our data would support the Y-model structure proposed by Westhof et al. (1989), in which the 5S rRNA is made up of three independent structural domains.

*Loop Structures.* Cleavage of 5S rRNA by Rh(phen)$_2$phi$^{3+}$ occurs at the junctions between loop E and helix V, loop B and helix II, and loop C and helix III. Similarly, we have observed cleavage by the rhodium complex at the anticodon stem–loop region of tRNA$^{Phe}$ and tRNA$^{Asp}$ from yeast (Chow et al., 1992). The crystal structures of the two tRNAs reveal that the anticodon stem–loop regions are single-stranded, yet the bases in the loop continue stacking in an A-like helical manner (Kim et al., 1974; Quigley & Rich, 1976; Westhof et al., 1985). The major groove of these regions is opened due to the absence of base pair hydrogen bonds. A broadening of the major groove at analogous stem–loop junctions in the 5S rRNA would facilitate interactions with the rhodium complex.

Westhof et al. (1989) have proposed noncanonical base pairing of the types A-A, U-U and A-G in the internal E loop. However, the NMR data from Varani et al. (1989) is inconsistent with structures of loop E containing the proposed A-G mismatched base pairs. Instead, the NMR structure revealed that extensive stacking is conserved on loop E and, to some extent, at the stem–loop junction. We have shown that mutations on one side of the stem–loop structure can alter cleavage by Rh(phen)$_2$phi$^{3+}$ on the opposite strand of the loop. For example, the mutations A74C and A74G lead to changes in cleavage at residues A101, U102, and A103 and the mutations A100C or A101U lead to changes at residues U73 and A74. These results suggest that the internal E loop contains an intrinsic structure in which the two strands of the E loop interact in an intimate fashion. This interaction may be due either to unusual base pairing or to the stacking of the nucleotides following the helical structure of the stem.

Mutations in the C loop show effects similar to those of the E loop mutations. The double mutation U43A–C44G leads to a loss in cleavage by Rh(phen)$_2$phi$^{3+}$ at C39 and C34 and diminished cleavage at A32 and G44. The mutation A42C leads to even more significant changes in the C loop cleavage at residues A32, C34, C36, C39, and C44. These data are also consistent with an intrinsic structure for loop C which favors interaction with the rhodium complex. Mutations in loop C seem to have significant effects on the folding of the C loop and subsequent recognition by Rh(phen)$_2$phi$^{3+}$. It is likely, on the basis of tRNA results, that these stem–loop regions of the 5S rRNA have opened major grooves and stacked structures in the single-stranded regions which are recognized by the metal complex.

*Helix Structures.* Cleavage by Rh(phen)$_2$phi$^{3+}$ does not occur in the canonical helical regions of the 5S rRNA but rather at regions which display unusual base pairing or bulged residues. On the basis of chemical modification and enzymatic degradation, there is a bulge in helix III with two A residues. Interestingly, Weeks and Crothers (1991) have proposed that bulges of two or three (but not one) U residues widen the RNA major groove. Similarly, the bulged AA residues in the 5S rRNA may cause an opening of the major groove and therefore facilitate stacking interactions with Rh(phen)$_2$phi$^{3+}$. It is also noteworthy that the rhodium complex does not exhibit cleavage at the proposed single-nucleotide bulges at residues A83 and C63.

We have shown that cleavage in helix IV is dependent on the U-U mismatch but not the bulged A83. The deletion of the bulged residue A83 has no effect on the cleavage in the middle of helix IV at U80 and G81. In contrast, conversion of the mismatch to either an A-U or G-U base pair leads to

a loss in cleavage at both U80 and G81. This rhodium complex does not appear to target G-U mismatches, and we have not yet tested the interactions of $Rh(phen)_2phi^{3+}$ with mismatches of the A-A or A-G type. It seems that the structural distortion of the helix created by the U-U mismatch is sufficient to allow interactions with the metal complex. It is noteworthy that structural distortions in the major groove at a U-C mismatch are evident in the crystal structure of an RNA dodecamer (Holbrook et al., 1991). It is also interesting that the cleavage we observe is asymmetric about the U-U mismatch. Although the helix appears to be symmetrical on the basis of sequence composition, we observe strong cleavage only on one side of the U-U mismatch. Furthermore, when the flanking G81-C95 base pair is changed to a C81-G95 base pair, cleavage is enhanced at U80 and C81, but still no cleavage is observed on the opposite strand. The flanking sequences must be important in determining how the mismatched U residues interact.

*Structural Analysis of 5S rRNA Loop Region: Comparison of Chemical Probing and $Rh(phen)_2phi^{3+}$ Cleavage.* Romaniuk et al. (1988) and Westhof et al. (1989) have used chemical modifications, such as dimethyl sulfate and diethyl pyrocarbonate (Ehresmann et al., 1987), as well as enzymatic probing to examine in detail the specific structures in the loop regions of *Xenopus* oocyte 5S rRNA. The effects of mutations on the structural organizations of the B and C loops (Brunel et al., 1990) and the E loop (Leal de Stevenson et al., 1991) have also been considered. In the B loop, most of the nucleotides are accessible to chemical modification and susceptible to enzymatic degradation by single-stranded ribonucleases. The rhodium cleavage data would be consistent with an open, unstacked structure in this loop which is not targeted by the metal complex, with binding by $Rh(phen)_2phi^{3+}$ being limited instead to the stem–loop junction where stacking is evident.

In contrast, chemical modification studies reveal that loop C contains unreactive pyrimidine residues at U33, C34, U43, and C44. These residues likely stack inside the loop without making hydrogen-bonding contacts. Furthermore, it was proposed that the neighboring residues are base paired by a trans Hoogsteen arrangement (U35-A42) and a Watson–Crick arrangement (C36-G41) (Brunel et al., 1990). $Rh(phen)_2phi^{3+}$ may recognize such stacked structures within the C loop. Studies have shown that the rhodium complex promotes strand scission in the TΨC loop of tRNA, in which residues are intimately stacked (Chow et al., 1991). Changes in rhodium cleavage associated with the mutant U43A-C44G may be a result of changes in stacking of the purine residues (A43 and G44) inside the loop, since purines would stack differently than pyrimidines. Differences in cleavage in the C loop region for the mutant A42C may result from a loss of the proposed A42-U35 base pair which could also be important for maintaining stacking of the neighboring pyrimidine residues. The fact that the rhodium complex still cleaves in the C loop of mutant A42C, however, would suggest that the C loop is intrinsically structured. It is interesting to note that cleavage by $Rh(phen)_2phi^{3+}$ is symmetric about a structure represented by the helix

$$^{31}\text{GAUCUC}$$
$$\text{CUCUAG}^{41}$$

with mismatched pyrimidine bases and with recognition sites for $Rh(phen)_2phi^{3+}$ at its center.

Chemical modification studies have shown that the E loop is highly structured through noncanonical hydrogen-bonding interactions. As seen in the C loop, mutants which destroy the potential for hydrogen bonding in the E loop result in an increased reactivity to probes for chemical accessibility at residues 74–77 and 99–102 at both the Watson–Crick and the N7 positions (Leal de Stevenson et al., 1991). Here we have considered only single-nucleotide mutations which can alter the proposed base pairs in the E loop. Mutants A74C and A74G, which should disrupt the noncanonical base pairs in the E loop, show only slight enhancements in cleavage at U73 by $Rh(phen)_2phi^{3+}$ and diminished cleavage at residues 101–103 on the opposite strand. The overall patterns of cleavage by $Rh(phen)_2phi^{3+}$ are the same for both of these mutants. Similarly, the mutations A100C and A101U should alter the proposed base pairing schemes and cause structural deviations within the loop. However, the overall rhodium cleavage patterns are identical for these mutants, with enhancements in the cleavage intensities compared to cleavage on wild-type 5S rRNA. It seems that the stacking interactions in the loop are again more important than the hydrogen-bonding capabilities with respect to interaction with the metal complex. The proposed structure for loop E in wild-type 5S rRNA shows only slight distortions from an A-form helix (Westhof et al., 1989). However, we have shown previously that the metal complex cannot interact in the deep and narrow groove of an A-form double helix (Chow & Barton, 1990). On the basis of the recognition characteristics of $Rh(phen)_2phi^{3+}$, then, we would propose that the E loop has a significantly more open structure than an A-form helix in which the bases are stacked but not closely associated by hydrogen bonding. Mutations on one side of the stem–loop structure which alter cleavage by $Rh(phen)_2phi^{3+}$ on the opposite side demonstrate that even in the absence of base pair hydrogen bonds, the structure of the loop is determined by the close interaction of bases which are opposite one another. This could be a result of continued stacking from the helical regions of the molecule.

On the basis of the data described here and elsewhere, some general conclusions can be made about the structures in the loop regions. All the results support the notion that these regions contain unusual structures which are not purely double-helical or single-stranded. Loops C and E of the wild-type 5S rRNA are resistant to both single-strand-specific and double-strand-specific nucleases (Brunel et al., 1990; Leal de Stevenson et al., 1991). In addition, chemical modification studies reveal that the bases in the E and C loops are inaccessible to chemical probing. This lack of reactivity could be the result of unusual hydrogen bonding or close stacking in the strands which makes the bases inaccessible to solvent. Similarly, $Rh(phen)_2phi^{3+}$ exhibits strong cleavage in the loop regions of 5S rRNA. These data indicate that within both loops C and E the strands constituting each loop are not independent of one another but are intimately and intrinsically structured, either by noncanonical base pairing or by the stacking of the bases. Further studies are necessary to determine the exact structures of these regions.

*Implications for Protein Binding.* $Rh(phen)_2phi^{3+}$ targets unique sites on 5S rRNA which are neither double-helical nor single-stranded. Instead, the rhodium complex binds preferentially to regions of the molecule containing more complex tertiary structure in which the major groove has become open and accessible. A broadening of the major groove at stem–loop junctions facilitates interaction with the metal complex. Similarly, multiple bulged nucleotides and base pair mismatches in the helical regions appear to cause a widening of the major groove which better accommodates the rhodium complex.

This specific targeting of open, structured major grooves may correlate with site recognition by proteins which bind 5S rRNA. Recent studies have suggested that structural variations in the major groove of the RNA may be critical in making contacts with protein (Ruff et al., 1991; Weeks & Crothers, 1991). A recent crystal structure has revealed that yeast aspartyl-tRNA synthetase interacts with the end of the acceptor stem and at the anticodon stem–loop junction of $tRNA^{Asp}$ in the major groove (Ruff et al., 1991); this major groove interaction is made possible by the increased accessibility of the bases in a helix–loop junction. Similarly, a model for RNA–protein recognition developed by Weeks and Crothers (1991) involves the distortion of an A-form helix by bulged nucleotides, which permits protein binding in the opened major groove of the RNA.

Interestingly, regions of the 5S rRNA which are recognized by $Rh(phen)_2phi^{3+}$ appear to be critical for binding by the *Xenopus* transcription factor, IIIA (TFIIIA). TFIIIA binds to 5S rRNA in immature oocytes to form a ribonucleoprotein particle that stabilizes the nucleic acid until it is required for ribosome assembly (Picard & Wegnez, 1979; Pelham & Brown, 1980). TFIIIA is also one of three factors that must bind to the internal promoters of the 5S rRNA genes for proper initiation of transcription (Sakonju et al., 1980; Bogenhagen et al., 1980; Engelke et al., 1980). While TFIIIA interacts with a substantial portion of the 5S rRNA (Huber & Wool, 1986; Christiansen et al., 1987; Timmins et al., 1988; Darsillo & Huber, 1991), mutagenesis experiments reveal that specificity is conferred by several independent interactions dispersed over the RNA binding site that depend upon the higher order structure of the nucleic acid (Romby et al., 1990; You et al., 1991; Rawlings & Huber, 1992). On the basis of nuclease and chemical protection experiments (Christiansen et al., 1987) as well as through hydroxyl radical footprinting (Darsillo & Huber, 1991), it appears that the junction between helical stems and internal loops of 5S rRNA provide the primary binding sites for TFIIIA. Moreover, missing nucleoside experiments have established that the strands of loop E constitute an important recognition site for TFIIIA (Darsillo & Huber, 1991). Hence, a correlation is evident between the regions targeted by $Rh(phen)_2phi^{3+}$ and determinants for recognition by TFIIIA. The opened structures in the major groove, recognized in binding $Rh(phen)_2phi^{3+}$ may be similarly important to effect specific recognition by the protein. It is noteworthy in this context that on the 5S rRNA gene $Rh(phen)_2phi^{3+}$ appears to mark sites of binding of the individual fingers of TFIIIA (Huber et al., 1991). $Rh(phen)_2phi^{3+}$ may be generally useful in marking potential sites for protein recognition in the major groove of RNA molecules.

## References


Andersen, J., Delihas, N., Hanas, J. S., & Wu, C.-W. (1984) *Biochemistry 23*, 5752–5759.

Bogenhagen, D. F., Sakonju, S., & Brown, D. D. (1980) *Cell 19*, 27–35.

Böhm, S., Fabian, H., Venyaminov, S. Y., Matveev, S. V., Lucius, H., Welfle, H., & Filimonov, V. V. (1981) *FEBS Lett. 132*, 357–361.

Brunel, C., Romby, P., Westhof, E., Romaniuk, P. J., Ehresmann, B., & Ehresmann, C. (1990) *J. Mol. Biol. 215*, 103–111.

Calnan, B. J., Tidor, B., Biancalana, S., Hudson, D., & Frankel, A. D. (1991) *Science 252*, 1167–1171.

Chow, C. S., & Barton, J. K. (1990) *J. Am. Chem. Soc. 112*, 2839–2841.

Chow, C. S., Behlen, L. S., Uhlenbeck, O. C., & Barton, J. K. (1992) *Biochemistry 31*, 972–982.

Christiansen, J., Douthwaite, S. R., Christensen, A., & Garrett, R. A. (1985) *EMBO J. 4*, 1019–1024.

Christiansen, J., Brown, R. S., Sproat, B. S., & Garrett, R. A. (1987) *EMBO J. 6*, 453–460.

Darsillo, P., & Huber, P. W. (1991) *J. Biol. Chem. 266*, 21075–21082.

Engelke, D. R., Ng, S.-Y., Shastry, B. S., & Roeder, R. G. (1980) *Cell 19*, 717–728.

England, T. E., & Uhlenbeck, O. C. (1978) *Nature 275*, 560–561.

Ehresmann, C., Baudin, F., Mougel, M., Romby, P., Ebel, J.-P., & Ehresmann, B. (1987) *Nucleic Acids Res. 15*, 9109–9128.

Fox, G. E., & Woese, C. R. (1975) *Nature 256*, 505–506.

Göringer, H. U., & Wagner, R. (1986) *Nucleic Acids Res. 14*, 7473–7485.

Hancock, J., & Wagner, R. (1982) *Nucleic Acids Res. 10*, 1257–1269.

Holbrook, S. R., Cheong, C., Tinoco, I., Jr., & Kim, S.-H. (1991) *Nature 353*, 579–581.

Huber, P. W., & Wool, I. G. (1986) *Proc. Natl. Acad. Sci. U.S.A. 83*, 1593–1597.

Huber, P. W., Morii, T., Mei, H.-Y., & Barton, J. K. (1991) *Proc. Natl. Acad. Sci. U.S.A. 88*, 10801–10805.

Johnson, B. A., McClain, S. G., Doran, E. R., Tice, G., & Kirsch, M. A. (1990) *BioTechniques 8*, 424–429.

Johnson, M. T., Read, B. A., Monko, A. M., Pappas, G., & Johnson, B. A. (1986) *BioTechniques 4*, 64–70.

Kao, T. H., & Crothers, D. M. (1980) *Proc. Natl. Acad. Sci. U.S.A. 77*, 3360–3364.

Kim, S. H., Sussman, J. L., Suddath, F. L., Quigley, G. J., McPherson, A., Wang, A. H. J., Seeman, N. C., & Rich, A. (1974) *Proc. Natl. Acad. Sci. U.S.A. 71*, 4970–4974.

Kime, M. J., & Moore, P. B. (1982) *Nucleic Acids Res. 10*, 4973–4983.

Leal de Stevenson, I., Romby, P., Baudin, F., Brunel, C., Westhof, E., Ehresmann, C., Ehresmann, B., & Romaniuk, P. J. (1991) *J. Mol. Biol. 219*, 243–255.

Luehrsen, K. R., & Fox, G. E. (1981) *Proc. Natl. Acad. Sci. U.S.A. 78*, 2150–2154.

Milligan, J. F., Groebe, D. R., Witherell, G. W., & Uhlenbeck, O. C. (1987) *Nucleic Acids Res. 15*, 8783–8798.

Mougel, M., Eyermann, F., Westhof, E., Romby, P., Expert-Bezancon, A., Ebel, J.-P., Ehresmann, B., & Ehresmann, C. (1987) *J. Mol. Biol. 198*, 91–107.

Nazar, R. N. (1991) *J. Biol. Chem. 266*, 4562–4567.

Peattie, D. A. (1979) *Proc. Natl. Acad. Sci. U.S.A. 76*, 1760–1764.

Peattie, D. A., & Gilbert, W. (1980) *Proc. Natl. Acad. Sci. U.S.A. 77*, 4679–4682.

Peattie, D. A., Douthwaite, S., Garrett, R. A., & Noller, H. F. (1981) *Proc. Natl. Acad. Sci. U.S.A. 78*, 7331–7335.

Pelham, H. R. B., & Brown, D. D. (1980) *Proc. Natl. Acad. Sci. U.S.A. 77*, 4170–4174.

Picard, B., & Wegnez, M. (1979) *Proc. Natl. Acad. Sci. U.S.A. 76*, 241–245.

Pieler, T., & Erdmann, V. A. (1982) *Proc. Natl. Acad. Sci. U.S.A. 79*, 4599–4603.

Pyle, A. M., Long, E. C., & Barton, J. K. (1989) *J. Am. Chem. Soc. 111*, 4520–4522.

Pyle, A. M., Morii, T., & Barton, J. K. (1990) *J. Am. Chem. Soc. 112*, 9432–9434.
Quigley, G. J., & Rich, A. (1976) *Science 194*, 796–806.
Rawlings, S. L., & Huber, P. W. (1992) (submitted for publication).
Romaniuk, P. J., Leal de Stevenson, I., Ehresmann, C., Romby, P., & Ehresmann, B. (1988) *Nucleic Acids Res.* 16, 2295–2312.
Romby, P., Baudin, F., Brunel, C., Leal de Stevenson, I., Westhof, E., Romaniuk, P. J., Ehresmann, C., & Ehresmann, B. (1990) *Biochimie 72*, 437–452.
Rould, M. A., Perona, J. J. Söll, D., & Steitz, T. (1989) *Science 246*, 1135–1142.
Ruff, M., Krishnaswamy, S., Boeglin, M., Poterszman, A., Mitschler, A., Podjarny, A., Rees, B., Thierry, J. C., & Moras, D. (1991) *Science 252*, 1682–1689.
Sakonju, S., Bogenhagen, D. F., & Brown, D. D. (1980) *Cell 19*, 13–25.
Silberklang, M., Gillum, A. M., & RajBhandary, U. L. (1977) *Nucleic Acids Res. 4*, 4091–4108.
Timmins, P. A., Langowski, J., & Brown, R. S. (1988) *Nucleic Acids Res. 16*, 8633–8644.
Varani, G., Wimberly, B., & Tinoco, I., Jr. (1989) *Biochemistry 28*, 7760–7772.
Weeks, K. M., & Crothers, D. M. (1991) *Cell 66*, 577–588.
Westhof, E., Dumas, P., & Moras, D. (1985) *J. Mol. Biol. 184*, 119–145.
Westhof, E., Romby, P., Romaniuk, P. J., Ebel, J.-P., Ehresmann, C., & Ehresmann, B. (1989) *J. Mol. Biol. 207*, 417–431.
You, Q., Veldhoen, N., Baudin, F., & Romaniuk, P. J. (1991) *Biochemistry 30*, 2495–2500.

# Characterization of the Heparin-Binding Site of Glia-Derived Nexin/Protease Nexin-1

Giorgio Rovelli,[‡] Stuart R. Stone,[§] Angelo Guidolin,[∥] Jürg Sommer,[⊥] and Denis Monard*
*Friedrich Miescher-Institut, P.O. Box 2543, CH-4002 Basel, Switzerland*
*Received October 15, 1991*

ABSTRACT: The interaction of heparin with glia-derived nexin (GDN) has been characterized and compared to that observed between heparin and antithrombin III (ATIII). Heparin was fractionated according to its affinity for immobilized GDN, and the ability of various fractions to accelerate the inhibition rate of thrombin by either GDN or ATIII was examined. Fractions with different affinities for GDN accelerated the thrombin–GDN reaction to a similar extent; heparin with a high affinity for immobilized GDN stimulated the reaction only about 30% more than the fraction that did not bind to immobilized GDN. Slightly greater differences were observed for the effect of these fractions on the thrombin–ATIII reaction; heparin that did not bind to the GDN affinity column was about 60% more effective than heparin with a high affinity for GDN in accelerating the inhibition of thrombin by ATIII. The CNBr fragment of GDN between residues 63 and 144 was able to reduce the heparin-accelerated rate of inhibition of thrombin by GDN indicating that this region of GDN was able to bind the heparin molecules responsible for the acceleration. Shorter synthetic peptides within this sequence did not significantly reduce the rate, suggesting that the heparin-binding activity of fragment 63–144 depends on a specific conformation of the polypeptide chain. Fragment 63–144 was less effective in decreasing the heparin-accelerated rate of inhibition of thrombin by ATIII. The results are discussed in terms of the heparin species that are responsible for the acceleration of the GDN– and ATIII–thrombin reactions and the heparin-binding sites of GDN and ATIII.

Glia-derived nexin (GDN)[1] is a 43-kDa secreted glycoprotein that can promote neurite elongation in neuroblastoma cells (Guenther et al., 1985) and in neuronal primary cultures (Zurn et al., 1988; Farmer et al., 1989). In vitro, GDN is secreted by primary cultures of rat brain origin (Schürch-Rathgeb & Monard, 1978; Rosenblat et al., 1987). In vivo, it has been shown to be expressed at high levels in the rat olfactory system (Reinhard et al., 1988) and lesions of the sciatic nerve were also found to induce a transient overexpression of GDN (Meier et al., 1989). GDN was first isolated from the conditioned medium of rat C6 glioma cells (Guenther et al., 1985). cDNA cloning and sequencing have shown that GDN and protease nexin-1[2] are identical proteins (Gloor et al., 1986; McGrogan et al., 1988). GDN is a member of the serpin (serine protease inhibitor) superfamily. It is a fast-acting inhibitor of thrombin and it also efficiently inhibits plasminogen activators and other trypsin-like proteases at a slower rate (Scott et al., 1985; Stone et al., 1987). Since

* Correspondence should be addressed to this author at the Friedrich Miescher-Institut, P.O. Box 2543, CH-4002 Basel, Switzerland.
[‡] Present address: Department of Neurobiology, Stanford University School of Medicine, Stanford, CA 94305-5401.
[§] Present address: Department of Haematology, University of Cambridge, MRC Centre, Hills Road, Cambridge CB2 2QH, U.K.
[∥] Present address: Department of Clinical Immunology, Flinders Medical Center, Bedford Park, South Australia 5042, Australia.
[⊥] Present address: Carlsberg Laboratory, Department of Physiology, DK-2500 Copenhagen-Valby, Denmark.

[1] Abbreviations: GDN, glia-derived nexin; ATIII, antithrombin III; pNA, *p*-nitroaniline; Pip, pipecolyl; TFA, trifluoroacetic acid.
[2] Since glia-derived nexin and protease nexin-1 are identical proteins, the abbreviation GDN is used to indicate both molecules.

0006-2960/92/0431-3542$03.00/0 